Available online at www.sciencedirect.com

ScienceDirect

Procedia Manufacturing 55 (2021) 116–123

Procedia MANUFACTURING

www.elsevier.com/locate/procedia

30th International Conference on Flexible Automation and Intelligent Manufacturing (FAIM2021)
7-10 September 2021, Athens, Greece.

Quality Prediction of Continuous Ultrasonic Welded Seams of High-Performance Thermoplastic Composites by means of Artificial Intelligence

D. Görick[a,]*, L. Larsen[a], M. Engelschall[a], A. Schuster[a]

[a]*German Aerospace Center (DLR), Center for Leightweight Production Technology, Am Technologiezentrum 4, 86159 Augsburg, Germany*

* Corresponding author. Tel.: +49-821-319874-1052 ; *E-mail address:* Dominik.Goerick@dlr.de

Abstract

Thermoplastic composites (TCs) are a famous choice when it comes to high performance designs for industrial applications. Since the growing demand on the use of this material, it is important to be able to evaluate suitable processing technologies. One of those technologies is continuous ultrasonic welding (CUSW) which creates continuous joints, also called seams, between two or more TCs parts. In CUSW mechanical oscillations are applied to the material and result in melting and connecting of the welding parts.
The approach to predict joint strength (qualities) of continuous ultrasonic welded TCs by training different neural networks is investigated in this study. Quality class prediction around 72 % accuracy is achieved with a fully connected neural network. Concluding, quality prediction of welded TCs with the help of artificial intelligence seems to be a suitable approach for quality observation but more research could lead to more reliable neural networks for industrial applications.

Keywords: Continuous Ultrasonic Welding; Thermoplastic Composites; Inline Process Monitoring; Artificial Intelligence; Neural Network; Deep Learning; 1DCNN

1. Introduction

Thermoplastic composite (TC) materials have grown on popularity since they are used in automotive and aerospace applications and other fields of engineering [1]. In addition to the wide use in industry, TCs have many different advantages as for example a better strength- and stiffness-to-weight ratio (in comparison to metal) [2, 3]. Another major advantage of thermoplastics is their weldability. However, own assumptions lead to the conclusion that the use of welding processes in industry is easier to accomplish if the process and the quality can be reliably monitored during production steps.

There are already some approaches to predict bonding qualities of ultrasonic welded TCs based on process observations. One research group investigated power- and displacement curves in order to be able to monitor the welding process and make assumptions about the produced welding quality [4]. Another research group developed a wave transmission model for predicting a weld quality class out of three [5]. This prediction model reached error rates in its prediction between 2 % and 42 %, depending on the setup [5]. Beside these two research groups there are other groups which investigate welding parameters and their influence [6] which underlines the importance of this topic.

All these researches seem to focus on the basic understanding of the welding process in order to deduce from this knowledge to weld quality or a better parameterization of the welding process. The use of an artificial intelligence (AI) to predict the bonding quality of continuous ultrasonic welded thermoplastic composites is, to the authors knowledge, a new approach and first preliminary tests indicate that this new method could lead to an accurate prediction method [7].

10.1016/j.promfg.2021.10.017

This work will investigate the quality prediction approach of continuous ultrasonic welded seams of TCs by using artificial intelligence and process data. For this investigation different types of process data (sequential- and single values) are measured and processed. The different data types lead to the necessity to use the Keras implemented functional API which is able to combine different neural networks and allows multiple inputs and outputs [8]. For sequential data a 1D-convolutional neural network (1DCNN) and for single values a fully connected neural network (FCNN) is used. In order to see if the prediction quality of a single FCNN is weaker, equal or better than the API approach, the sequential values are transformed into single values and fed to a FCNN.

All described experiments and results were created at the German Aerospace Center (DLR) at the Center for Lightweight Production Technology in the city of Augsburg [9].

Going further in this study, the theoretical background about ultrasonic welding and artificial intelligence will be described. After that, a paragraph about the experimental procedure of this work follows. Later on, the results of the network training- and testing phase are shown and summarized in a conclusion.

2. Theoretical Knowledge

2.1. Ultrasonic Welding

Ultrasonic welding (USW) and continuous ultrasonic welding (CUSW) are considered as good joining techniques for TCs [10, 11]. In the following subsection a description of USW takes place. It has to be considered that the general mechanisms of CUSW are the same than in USW [10].

In the process of USW an electrical signal with a 20-50 kHz frequency [12, 13] is transformed in mechanical oscillations [2, 11, 13] with 10-250 µm amplitudes [13]. The mechanical oscillations are transferred with a sonotrode into the welding parts [2, 11]. The necessary heat for the joining of the welding parts results from internal damping [12] or, more specific, form surface friction between the two welding parts and intermolecular friction [5]. A mathematical description of the internal heating process can be found in Appendix A. It is possible to place an energy director (ED) between two welding parts in order to focus the oscillations and create a smaller area where the heat is generated [14]. Figure 1 shows a schematic setup of the used ultrasonic welding setup.

The term continuous ultrasonic welding is applied when the seam is not consisting of single welded spots but of one continuous seam [13].

2.2. Artificial Intelligence

Artificial intelligence has different definitions in literature [8, 15]. For the purpose of this work it is adequate to understand AI as a designed, rational thinking agent which has to perform some kind of thinking process in order to solve a specific, cognitive task [15].

A subfield of AI is called machine learning where algorithms get labeled data and learn rules to describe the correlation between the data and its labels [8]. Goal of machine learning is that the learned rules can be applied to new data in order to make decisions about suitable labels [8].

If the representation of the data is learned by stacked layers of neurons, a neural network (NN) has been created and the term deep learning is used [8]. Neurons in different layers propagate an input signal form one neural layer up to the next neural layer [8, 16]. During the learning process of the NN, different weights of the connections between the neurons evolve and the algorithm learns how to connect the input to its fitting output [8, 16].

Since FCNNs and 1DCNNs are programmed in this work, the algorithms are settled in the category of deep learning.

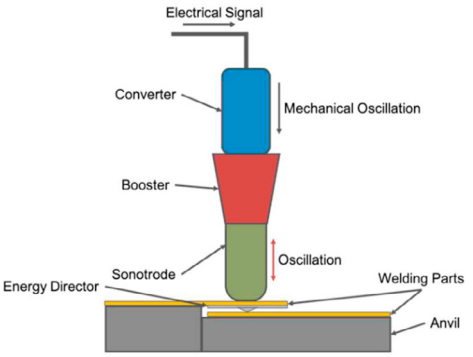

Figure 1: Scheme of the welding apparatus. An electrical signal is changed by a converter (blue) and a booster (red) in mechanical oscillations and used for welding two plates together. Figure inspired by descriptions of Bhudolia et al. [2].

2.3. Network Types

A FCNN can be seen as the basic network architecture of a deep learning algorithm. As displayed in Figure 2, stacked layers of neurons are used to build such a FCNN. Each neuron in a layer is connected to each neuron in the previous and following layer. These connections have each an initial weight which is changed during a learning process in order to produce the right output for given input data. In which way the weights are changed is regularized by a loss function which describes the error rate of the network in the prediction of outputs. The accuracy in the prediction of the network is maximized and the network learns, when the loss function is minimized. FCNNs are able to process multiple single input values. Since NNs calculate tensor operations, a single input value could be seen as zero-dimensional input. Figure 2 (a) shows the scheme of the basic structure of a FCNN. [8, 16]

1DCNNs are able to process one-dimensional input, as for example a measurement of a parameter over a period of time. In comparison to the architecture described above, 1DCNNs do not have single connected neurons but process the given input signals by convolving the signals with filters. Here, the weights in the filters are changed in order to give the 1DCNN the ability to learn. [8]

Figure 2 (b) shows the working mechanism of a 1DCNN. A real 1DCNN usually has different kinds of layers (see Figure 5 and Figure 6 in Appendix B) and not only convoluting ones.

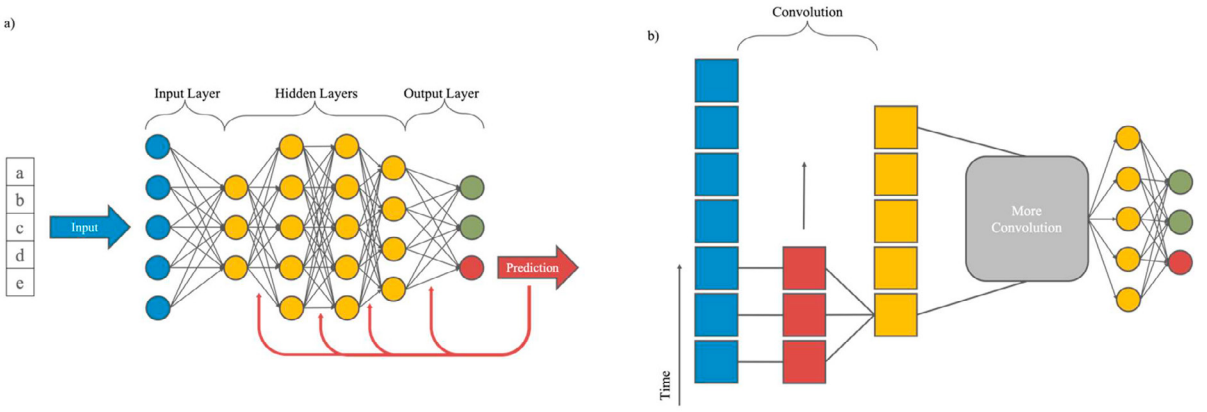

Figure 2: a) Scheme of FCNN. a-e represent five single input values which enter the FCNN over the input layer (blue). Together the input values are one-dimensional while each value represents another welding/process parameter. The data is processed in the hidden layers (yellow) and an output is produced (green/ red). The output layer shows the label decision (prediction) of the FCNN (red). A loss function changes the weights on the single neuron connections dependent on the right/ wrong decision of the FCNN during the training (red arrows). b) Scheme of a 1DCNN. One sequential input (here: one parameter measurement over time) is given to the algorithm (blue). A filter convolves the signal with a predefined size (red) and the results of the convolution are saved in a feature map (yellow). The filter runs over the length of the time sequence (grey arrow). The data can run through several convolutions and other processing layers (grey) until the data is fed to neurons which make a label prediction (yellow and green, label prediction red). Both figures are inspired by descriptions of Chollet [8].

3. Experimental Work & Methods

3.1. Design and Evaluation of the Welding Process

In order to get a NN which classifies data correctly, training of the NN is essential. Real TCs plates have to be welded for the generation of appropriate training data. During the welding of different samples, important welding parameters have to be varied so that good and bad welds can be fed to the NN. As welding material Toray Cetex® TC1225 with a carbon fiber orientation of $[(0/90)_3]_s$ is used. The fibers are embedded in a low melt PolyAkrylEtherKetone (LM-PAEK) matrix. The 1.8 mm thick and 500*500 mm wide plates are buzz sawed in 250.1*104 mm samples. One up to four EDs consisting of LM-PAEK with 60 to 200 µm thickness each, are placed between the welding plates. The plates and EDs are stored for at least 12 h at 60 °C and 0 %rH (relative humidity) before the welding takes place. For the welding process the plates are fixed with a 12.7 mm overlap (Figure 3) on an anvil. The here created overlap is equal to the area which connect the upper with the lower plate after the welding took place. CUSW is then performed by an end effector which was designed at the DLR [10] and mounted on a KUKA KR300 R2500 Ultra Robot. The spherical shaped sonotrode (welding surface dimension of ∅25 mm) is powered by a 20 kHz Branson generator while the process data of the welding is measured by a flied bus system which is able to record the measuring parameters with a frequency of 1 kHz. After the completed welding process the plates are water jet cut in 25.4 mm wide samples. With this procedure each welded plate is divided into nine samples for quality evaluation and one extra sample for other documentary purpose. For the experiments which are performed in this work 486 samples are used. In order to have a variety of welding setups covered, three design of experiments with weld forces between 400-900 N, amplitudes over 90 % (referred to the maximal output), welding velocities of 18-24.75 mm/s, consolidation pressure of 0.4-1.0 MPa, compaction roll (wheel unit which runs over the area which should be welded) force of 100-750 N and combined ED thicknesses of 120 µm (2*60), 200 µm (2*100 or 1*200) and 240 µm (4*60) are made. Caused to the limited availability of the welding material some older welding results are reused for these experiments (13 welds, process parameters are in the ranges which are described above).

Quality evaluation of the welded joints is done by lab shear strength (LSS) tests. The tests are performed as described in the ASTM D1002 norm. Cross head speed during the tests is set to 1.3 mm/min with a cross head starting distance of 80 mm. Shear strength was saved for each sample in the unit MPa.

3.2. Data Production and Processing

Five process parameters of the welding process are recorded and fed to the NN. Namely these parameters are the:

- applied *welding force* [N]
- *amplitude output* of the Branson unit [%]
- *power output* for the welding process [W]
- *welding speed* of the tool center point (TCP) [mm/s]
- *pressure of the consolidation unit* [bar]

Additionally, three other parameters are added manually to each data set. The *layer thickness* describes the thickness of the applied EDs in µm and is supplemented by the *number of layers* [abs] with which the total ED thickness can be calculated. The *position of a sample* (1-9) in the welded plate has to be used in a later step.

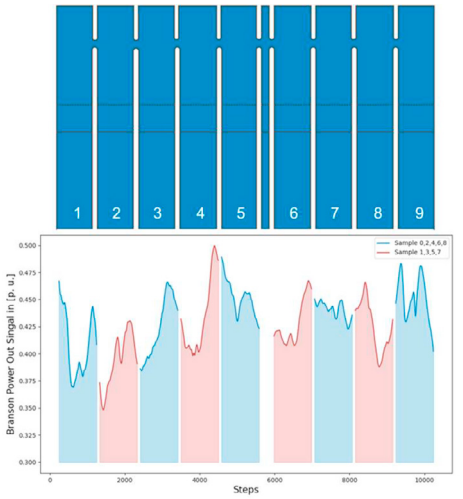

Figure 3: Upper part: Scheme of a welded plate with its division in lab shear strength test samples and one sample for documentary purpose (between 5 and 6). Lower part: Welding power (=Branson Power Out) signal which is divided in sub-samples which contain the values measured during the welding of each cut sample.

The recorded data are in their raw shape after the welding process. Preprocessing has to be done in order to make the data fit to the input layers of the different networks.

The first step of preprocessing the data is to create suitable labels for the data. If the task of the NN is to predict joint strength as continuous values, the measured LSS values are suitable for labeling the process data. In order to be able to make a quality prediction in terms of a quality class the LSS values have to get class labels. For this task the LSS values are divided in three quality classes. The first class contains all weld samples with an LSS value of 0 up to 15 MPa. The second class reaches from over 15 to 30 MPa and the last class stores all samples which have a joint strength of over 30 MPa.

The second step of preprocessing is to transform the data in order to bring them in the same range and similar shape. For this purpose, the data is normalized so that the parameter values range between 0 and 1. In the signal of the amplitude some measure points lay over 100 %. This measure points may occur because of irregularities in the measurement. Most of these outliers are nevertheless eliminated by the normalization process. In this process, the maximum of every process parameter is multiplied by 1.03 before dividing the whole data sequences by this value. Additionally, the moving average is calculated for each parameter measurement (window size of 31 measurement points). The moving average smooths the measurement and eliminates potentially edgy signals which may develop caused by the quantization of the process signals.

In the third step the sequential data of a welded plate is divided in the same sub-samples as the real plate is divided in (Figure 3). Each of these sub-samples gets a position tag which describes the relative position of the sample in the plate. The tags range from one to nine and were added in their normalized shape to the sequential sub-sampled data. Some of the measured parameters are steady values (e.g. velocity) or have a mean standard deviation near zero. From all these constant or nearly constant parameters the mean value over their sub-samples is calculated and taken as single input value for the training process. The parameters ‘Welding Force’ and ‘Welding Power’ are taken as sequential values.

The data storage contains 486 single LSS values and quality classes at the end of the preprocessing. Connected to these values, 486 files are stored which contain measured process parameters and manually added process information which should either be processed as a single value or a sequential value.

3.3. Network Architectures

Besides the libraries Keras and TensorFlow, matplotlib, pandas and numpy are used for the programming tasks. All programming is done in Python (3.6.8).

Four different network architectures were designed in order to perform quality class label prediction (classification) and LSS value prediction (regression). The use of an API makes it possible to feed a network with single and sequential values of a sample at the same time. For this purpose, a 1DCNN is designed to take the sequential input and a FCNN is supposed to compute the single values. Both NNs create the input for a final FCNN which should create the final prediction of a class label or a joint strength. Single FCNNs are designed for investigating the importance of the chosen sequential values and the necessity of a 1DCNN. The mean values of all parameters are calculated for the single FCNN approach. Both architectural approaches are shown in Figure 4.

Independent of the network architecture, k-fold cross validation (k=4) was performed with each network in order to reduce the overfitting and to create a more generalized model [17]. Not every sequence of the sequential values has the same length. Since the layer dimensions are fixed parameters, the network cannot take different sequence length as input. Due to this, shorter sequences are filled at the end with zeros so all fed sequential data has the same length.

Each network is trained and validated (cross validation) with a data size of 386 samples (290 training, 96 validation) in order to hyper parameterize the network. Afterwards the final networks are trained with 386 and tested with 100 samples. The samples are randomly divided in a training/ validation and a testing data set. Of all 486 samples 41.98 % have a joint strength >30 MPa, 32.51 % lie between >15 and <=30 MPa and 25.51 % belong to the quality group of <=15 MPa.

The specific designs of each network are shown in Figure 5 and Figure 6 in Appendix B. The API network which performs regression uses the Adam optimizer and has a learning rate of 0.001. The other API for the classification task used the Adamax optimizer with a learning rate of 0.002. The FCNN uses the Adagrad optimizer with a learning rate of 0.02 for predicting a continuous value while the last FCNN for the classification task uses the Adam optimizer with a learning rate of 0.001.

Dependent on the type and structure of the NN, different amounts of training epochs are necessary. The epoch number which leads to the best result during the architectural development of a network is taken as default setup for the final trainings. The term ‘best result’ is defined by a low mean

absolute error (mae) for the joint strength prediction task or a high prediction accuracy in terms of class prediction. The network is overfitted if the mae/ the prediction accuracy of the training phase is lower/ higher than the mae/ prediction accuracy of the test phase [8]. To observe the overfit of a network, the *delta* (Δ) of the training and the testing mae/ prediction accuracy is calculated and the number of training epochs is reduced with the goal to get the delta as closest to zero as possible.

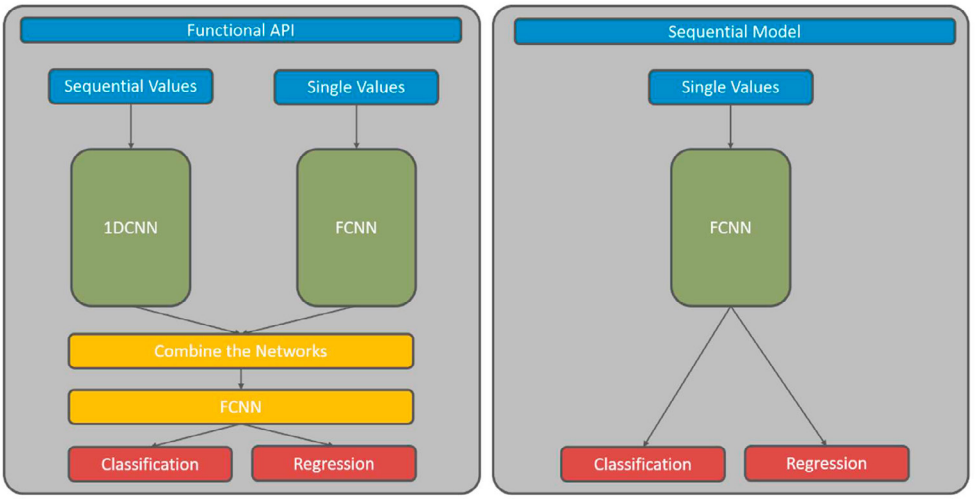

Figure 4: Schematic of the architectures of the developed NNs. Left: API approach with the possibility to have sequential input and single value input. Right: A model with can only take single value input. Both architectures are able to perform either a classification or a regression.

4. Results

The final training of the API network for the regression task is started with an epoch number of 290. Since the two mae values have a difference of nearly one, the epoch number is reduced to 50 which leads to a network with a smaller delta and a mae in joint strength prediction of around 5.44 MPa for new data (Table 1).

Table 1: Mae values of the API for the regression task. Units of mae and delta in [MPa]. Results from training (train) and testing (test) are listed.

epochs	mae train	mae test	Δ
290	3.777	4.742	0.965
190	4.061	5.187	1.126
90	4.959	5.323	0.364
50	5.402	5.435	0.033

The training process of the FCNN for the regression task starts with 776 trainings epochs. This starting point leads to a relatively high delta so the epoch number is reduced until the delta measures 0.040 and the network has a mae of 5.315 MPa for new data (Table 2).

The delta from the API with the classification task starts at -15.3 % with 124 training epochs. A reduction of the epoch number leads to bigger differences between training- and testing accuracy. In this case the overfitting cannot be reduced since the deltas are, according to amount, rising (Table 3).

Table 2: Mae values of the FCNN for the regression task. Units of mae and delta in [MPa]. Results from training (train) and testing (test) are listed.

epochs	mae train	mae test	Δ
776	3.506	4.308	0.802
600	3.971	4.492	0.521
400	3.955	4.268	0.313
200	5.275	5.315	0.040

Table 3: Accuracy (acc) of prediction values of the API for the classification task. Units of acc and delta in [%/100]. Results from training (train) and testing (test) are listed.

epochs	acc train	acc test	Δ
124	0.793	0.640	-0.153
100	0.782	0.590	-0.192
75	0.769	0.530	-0.239
50	0.712	0.480	-0.232

The FCNN has a prediction accuracy of quality classes of 68 % with an already small absolute delta of 2.5 % with a default setup of 394 training epochs. The best result in prediction accuracy is achieved with 300 training epochs and measures 72 %. The corresponding delta is +0.5 % (Table 4).

Table 4: Accuracy (acc) of prediction values of the FCNN for the classification task. Units of acc and delta in [%/100]. Results from training (train) and testing (test) are listed.

epochs	acc train	acc test	Δ
394	0.705	0.680	-0.025
350	0.720	0.660	-0.060
300	0.715	0.720	+0.005
250	0.668	0.680	+0.012

After the testing process of the four developed networks the FCNN with a mae of 5.315 MPa makes the best joint strength predictions and the FCNN with a prediction accuracy of quality classes of 72 % deliver the best and most reliable results.

5. Conclusion

In the experiments the FCNN for the classification task achieved a class prediction accuracy of 72 % which is the best outcome so far. If this prediction value is compared to randomly guessing the quality classes (33.33 % accuracy) the results are more than twice as good in their accuracy. The accuracy for randomly guessing results from the thought that there are three classes with an unknown distribution which results in 33.33 % accuracy. Hypothetically it is possible to guess always the same class, so possible accuracy values are 25.51 (samples <=15 MPa), 32.51 (samples between >15 and <=30 MPa) and 41.98 % (samples >30 MPa) (mean of 33.33 %) which is while for this conclusion 33.33 % is chosen as a value to compare the results with. Nevertheless, the prediction of joint strength has a minimal mae of 5.315 MPa which gives every prediction a relatively high tolerance. Despite this tolerance, the algorithms seem to respond to the given data in a positive way. It may be necessary to create more/ other input data in order to maximize the NNs prediction performance.

At the moment the use of an API with a 1DCNN and a FCNN has no advantage but leads to weaker prediction results. Other research teams report outstanding results with the use of 1DCNNs for computing sequential process data [17-21]. This fact leads to the conclusion that the used sequential data in this study seem to contain not enough information to train the NNs more accurately. In general, the training with other sequential or non-sequential data might lead to a more reliable network and has to be investigated.

Since the networks show a learning behavior, the attempt to predict the weld quality of continuous ultrasonic welded parts can be seen as a first success. Nevertheless, more investigations about which process data are used and in what shape they are given to the NNs are necessary in order to create a more reliable network. If a NN with a higher prediction accuracy is developed, it could supervise the quality of continuous ultrasonic welded seams or even monitor and control the welding process in industrial applications. This work is the first step in the development of an in-line, non-destructive technique to evaluate the joining quality of CUSW TCs parts and therefore can lead to advanced approaches which enable the use of CUSW of TCs in industry.

CRediT author statement

Dominik Görick: Conceptualization, Methodology, Software, Investigation, Writing – Original Draft. Lars Larsen: Software, Writing – Review & Editing, Supervision. Manuel Engelschall: Resources, Investigation, Writing – Review & Editing. Alfons Schuster: Writing – Review & Editing.

Acknowledgement

This project has received funding from the Clean Sky 2 Joint Undertaking (JU) under grant agreement No 945583. The JU receives support from the European Union's Horizon 2020 research and innovation program and the Clean Sky 2 JU members other than the Union.

Disclaimer

The results, opinions, conclusions, etc. presented in this work are those of the author(s) only and do not necessarily represent the position of the JU; the JU is not responsible for any use made of the information contained herein.

Appendix A. Internal Heat Generation

A formula (Equation 1) which describes the internal heat generation (per unit time and per unit volume) during the ultrasonic welding process is mentioned in literature [22]:

$$\dot{Q}_{avg} = \frac{\omega E'' \varepsilon_0^2}{2} \quad (1)$$

The average internal heat generation $\dot{Q}_{avg}$ is here calculated with the operating frequency ω in the unit *rad/s,* the loss modulus E'' of the welded material and the strain amplitude ε_0 [22].

Appendix B. Network Designs

The following figures (Figure 5 and Figure 6) display the structural characteristics of the four designed networks. Here, it has to be noticed that the used convention is not equal to the way the NNs are programmed. The shown figures have only the purpose of visualizing the general structure.

For the creation of the figures most of the common names of the Keras library are used. The layer type is always written in front of the brackets. The brackets contain further information about the configuration of a single layer. For further details about the different layer types and their functionalities read [8, 9].

Figure 5 (a) shows the schematic structure of the used API for the regression task. On the left-hand side the structure of the 1DCNN is displayed. Here, convolving- and pooling layers are used in order to process given sequential data. At the end of the 1DCNN a flatten layer is used before the data enters the FCNN which makes the quality prediction. On the

right-hand side the structure of the FCNN is displayed. This network is built by dense layers. The FCNN is connected to the same FCNN as the 1DCNN in order to merge the data processing together in one network. The final FCNN creates an output based on the data from the previous two networks. In the last layer no activation function is used and a continuous value is generated as output of this network.

In Figure 5 (b) the architecture of the FCNN for the regression task is displayed. Except of one dropout layer, this network is built by dense layers only. Similar to the API, the last layer has no activation function.

Figure 6 (a) shows the API network for the classification task. Similar to the API for the regression task, the API for the classification is built with a 1DCNN consisting of convolutional- and pooling layers and a FCNN with dense layers. Both networks merge their data in a final FCNN which makes the class prediction. This prediction is made by an activation function in the last layer.

Figure 6 (b) displays the setup of the FCNN for the classification task. This network is built by similar layers than the FCNN for the regression task but has an activation function in its output layer.

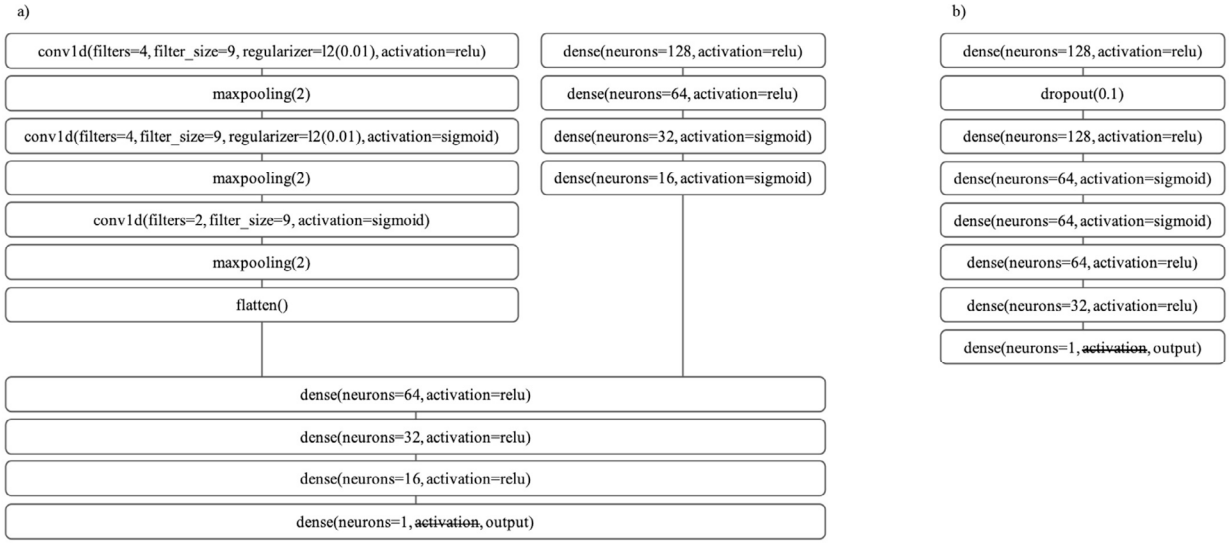

Figure 5: a) Structure of the API for the regression task. On the left-hand side, the structure of the 1DCNN is displayed which processes the sequential values. On the right-hand side is the structure of the FCNN for taking the single values as input. Both network outputs are combined in a final network which generated the output (prediction of joint strength in MPa) b) Structure of the FCNN for the regression task.

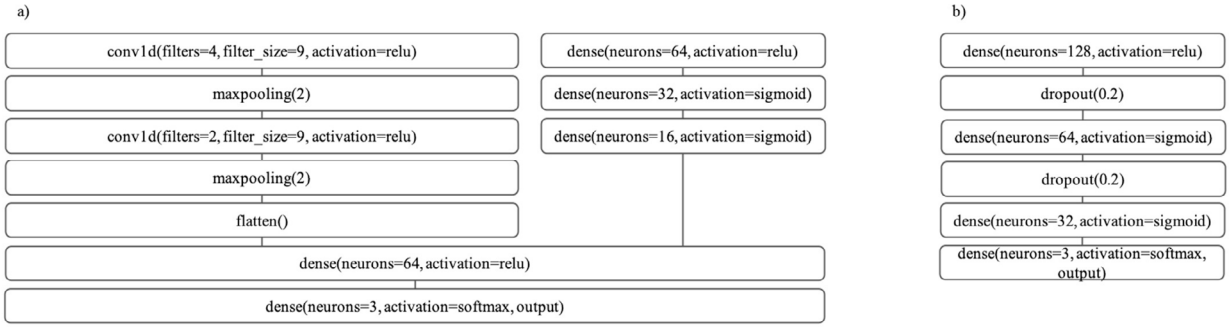

Figure 6: a) Structure of the API for the classification task. On the left-hand side, the structure of the 1DCNN is displayed which processes the sequential values. On the right-hand side is the structure of the FCNN for taking the single values as input. Both network outputs are combined in a final network which generated the output (prediction of a quality class) b) Structure of the FCNN for the classification task.

References

[1] Lässig R, Eisenhut M, Mathias A, Schulte R T, Peters F, Kühmann T, Waldmann T, Begemann W. *Series production of high-strength composites: Perspectives of the German engineering industry*. Roland Berger Strategy Consultants, VDMA; 2012

[2] Bhudolia S K, Gohel G, Leong K F, Islam A. Advances in Ultrasonic Welding of Thermoplastic Composites: A Review. *Materials* 2020; 13(6): 1284 1-26.

[3] Yousefpour A, Hojjati M, Immarigeon JP. Fusion Bonding/Welding of Thermoplastic Composites. *Journal of Termoplastic Composite Materials* 2004; 17(4): 303-341.

[4] Villegas I F. In situ monitoring of ultrasonic welding of thermoplastic composites through power and displacement data. *Journal of Thermoplastic Composite Materials* 2015; 28(1): 66-85.

[5] Li Y, Liu Z, Shen J, Lee T H, Banu M, Hu S J. Weld Quality Prediction in Ultrasonic Welding of Carbon Fiber Composite Based on an Ultrasonic Wave Transmission Model. *Journal of*

Manufacturing Science and Engineering 2019; 141(8): 081010-1-081010-15.

[6] Wang K, Shriver D, Li Y, Banu M, Hu S J, Xiao G, Arinez J, Fan HT. Characterization of weld attributes in ultrasonic welding of short carbon fiber reinforced thermoplastic composites. *Journal of Manufacturing Processes* 2017; 29: 124-132.

[7] Larsen L, Görick D, Engelschall M, Fischer F, Kupke M. Process Data Driven Advancement of Robot-Based Continuous Ultrasonic Welding. *ITHEC 2020, Messe Bremen* 2020; 1-4.

[8] Chollet F. *Deep Learning mit Python und Keras: Das Praxis-Handbuch vom Entwickler der Keras-Bibliothek*. Frechen: mitp Verlags GmbH & Co. KG; 2018.

[9] Görick D. *An Artificial Intelligence Approach for the Joint Strength Prediction of Continuous Ultrasonic Welds of High Performance Thermoplastic Composites*. German Aerospace Center; 2020.

[10] Engelschall M, Larsen L, Fischer J C F, Kupke M. Robot-based Continuous Ultrasonic Welding for Automated Production of Aerospace Structures. *SAMPE Europe Conference 2019 Nantes – France* 2019; 1-8.

[11] Villegas I F, Bersee H E N. Ultrasonic Welding of Advanced Thermoplastic Composites: An Investigation on Energy-Directing Surfaces. *Advances in Polymer Technology* 2010; 29(2): 112-121.

[12] Nonhof C J, Luiten G A. Estimates for Process Conditions During the Ultrasonic Welding of Thermoplastics. *Polymer Engineering and Science* 1996; 36(9): 1177-1183.

[13] Villegas I F. Ultrasonic Welding of Thermoplastic Composites. *Frontiers in Materials* 2019; 6: 1-10.

[14] Webpage: *Joint Designs for Ultrasonic Welding*. Sonics & Materials, Inc. Link: https://www.sonics.com/site/assets/files/2951/joint-designs-for-ultrasonic-welding.pdf. (Accessed: 17.04.2020).

[15] Sewak M. *Deep Reinforcement Learning: Frontiers of Artificial Intelligence*. Singapore: Springer Nature Singapore Pte Ltd.; 2019.

[16] Rashid T. *Neuronale Netze selbst programmieren: Ein verständlicher Einstieg mit Python*. Heidelberg: dpunkt.verlag GmbH, O´Reilly; 2017.

[17] Eren L, Ince T, Kiranyaz S. A Generic Intelligent Bearing Fault Diagnosis System Using Compact Adaptive 1D CNN Classifier. *Journal of Signal Processing Systems* 2019; 91: 179-189.

[18] Cho H, Yoon S M. Divide and Conquer-Based 1D CNN Human Activity Recognition Using Test Data Sharpening. *Sensors* 2018; 18(4): 1055 1-24.

[19] Ince T, Kiranyaz S, Eren L, Askar M, Gabbouj M. Real-time motor fault detection by 1-D convolutional neural networks. *IEEE Transactions on Industrial Electronics* 2016; 63(11): 7067-7075.

[20] Kiranyaz S, Ince T, Gabbouj M. Real-time patient-specific ECG classification by 1-D convolutional neural networks. *IEEE Transactions on Biomedical Engineering* 2015; 63(3): 664-675.

[21] Startsev M, Agtzidis I, Dorr M. 1D CNN with BLSTM for automated classification of fixations, saccades, and smooth pursuits. *Behavior Research Methods* 2019; 51: 556-572.

[22] Grewell D. A., Benatar A. and Park J. B. Ultrasonic Welding. In: *Plastics and composites welding handbook*. (Grewell D. A., Benatar A. and Park J. B.) 1st ed., 407 pages, Munich: Hanser-Cincinnati: Hanser Gardener; 2003.